

Effect of the Cassie Baxter-Wenzel behaviour transitions on the corrosion performances of AA6082 superhydrophobic surfaces

A. Khaskhoussi, L. Calabrese, E. Proverbio

Turning the wetting behaviour of a solid surface from hydrophilic to hydrophobic by making morphological and chemical modifications has attracted great attention over the past few years due to the importance of these surfaces in fundamental research and industrial applications in particular for anti-corrosion purpose. In this work, a chemical etching-based approach, which can be easily scaled to industrial level, was proposed to obtain super-hydrophobic surfaces on 6082-T6 aluminium plates. The results showed that the wetting transitions from Cassie-Baxter to Wenzel regime and vice versa can be controlled by changing the etching time. The mechanism at the basis of the wetting behaviour is based on the nanostructure roughness. In addition, the as-prepared aluminium surfaces revealed a good corrosion resistance behaviour in seawater compared with the as received one. The relationships between the corrosion performances and the Cassie Baxter-Wenzel behaviour transitions were deeply discussed.

KEYWORDS: HYDROPHOBICITY, CASSIE-BAXTER, WENZEL, ALUMINIUM ALLOY, CORROSION, CHEMICAL ETCHING

INTRODUCTION

Wetting behaviour is an important characteristic in surface chemistry, and it can be roughly distinguished into hydrophobic and hydrophilic. Current achievements in the fabrication of synthetic surfaces for special degrees of wettability are typically focused on super-hydrophobicity. Superhydrophobic surfaces are characterised by a water contact angle (WCA) higher than 150° and a water sliding angle (WSA) lower than 10° . These surfaces have recently drawn significant attention because they have a wealth of applications starting from day-to-day activities to health care. Some of these applications include but are not limited to condensation enhancement [1], anticorrosion [2,3], drug delivery [4] and self-cleaning [5]. The superhydrophobicity behaviour is mainly governed by the surface morphology (roughness) and the surface chemical composition which requires deep fundamental understanding [6].

The contact angle (CA) of a liquid on a chemically homogeneous and flat solid surface is calculated according to the

Amani Khaskhoussi

National Interuniversity Consortium of Materials Science and Technology, INSTM, Firenze, Italy, corresponding author:
khaskhoussiamani105@gmail.com

Luigi Calabrese, Edoardo Proverbio

Department of Engineering, University of Messina, Messina, Italy, lcalabrese@unime.it, eproverbio@unime.it

Young's equation:

$$(1) \cos\theta = \frac{\gamma_{sg} - \gamma_{ls}}{\gamma_{lg}}$$

where γ_{lg} , γ_{sl} and γ_{sg} are respectively the liquid-gas, the solid-liquid and the solid-gas interfacial tensions. The maximum contact angle that can be obtained on a flat surface by reducing the surface energy is 120° [7]. In this concern, in order to reach an extreme CA it is obligatory to combine the low surface energy with a hierarchical rough structure [8]. Wenzel proposed a relationship between the surface roughness ratio (ratio of the rough surface area to the smooth surface one), and the ideal liquid contact angle (Θ), which is given as

$$(2) \cos\theta_w = r\cos\theta$$

where θ_w is the Wenzel's (or apparent) contact angle. According to this equation, by increasing the surface roughness, the hydrophilic surface becomes more hydrophilic and the hydrophobic surface becomes more hydrophobic. In the Wenzel state, the water droplets penetrate the rough surface cavities and show a high adhesion force. Such behaviour is known also as the homogeneous wetting state [9,10]. On the other hand, on some superhydrophobic surfaces, water does not fill the interstitial spaces formed by the hierarchical micro/nanostructures and easily roll-off the surface. This phenomenon is due to the entrapment of

air in such "pockets", which governs the transition from the Wenzel to Cassie-Baxter state. According to Cassie-Baxter, the most part of the surface is separated by air cushions; thus, the interaction between the liquid and the solid surface is greatly reduced. The Cassie-Baxter CA on the solid-air composite surface is calculated according to the equation:

$$(3) \cos\theta_{CB} = f(r\cos\theta + 1) - 1$$

where f is the fraction of wetted area.

Therefore, depending on the surface roughness, different wetting states are possible that can meet a wide range of applications. Over the last decade, a large number of studies, involving numerous methods and materials, have focused on the fabrication of superhydrophobic surface [11]. Nevertheless, the use of such surfaces in industrial application needs deep control of the surface roughness in order to properly extend and enhance their applicability [6].

In the present work, a superhydrophobic surface was fabricated on aluminium substrate using a simple two-steps method. Micro/nano rough structures were achieved by acid etching, at different times, and the free energy of the surface was reduced using a thin silane film. The Cassie-Baxter to Wenzel regime transition was investigated. In addition, the effect of the etching time on the corrosion performances of the superhydrophobic aluminium surfaces have been studied.

MATERIALS AND METHODS

Metal substrates of EN AW-6082 T6 aluminium alloy measuring 30 mm x 24 mm were obtained from a 2 mm thick plate. Hydrochloric acid (37%) and Nitric acid (60%) were used for sample chemical etching. Octadecyltrimethoxysilane (90%) was used for low surface energy coating. All aluminium substrates were cleaned in ultrasonic bath with ethanol, acetone and ultra-pure water, and finally drying at room temperature. In order to produce hierarchical rough structure on the bare aluminium alloy surfaces, HNO₃/HCl chemical etching was applied according to the following process: the cleaned samples were etched with an HNO₃/HCl/H₂O acidic solution (ratio 1:3:2) at different times (10, 20, 40 and 60 minutes). Afterward, the etched samples were rinsed in an ultrasonic bath with ultra-pure water to remove residual acids and dried in oven at 70°C for 60 min. The etched aluminium samples were immersed in 0.1% by

weight solution of silane in toluene for 10 min. Finally, all substrates were treated for 3 hours at 100°C to complete the silane curing. The static water contact angles on the sample surface were measured, at room temperature, using an Attension Theta Tensiometer by Biolin Scientific according to the sessile drop technique. Ten replicas of water contact angle (WCA) and water sliding angle (WSA) for each sample were made. Morphological analysis of the prepared surfaces was performed using the scanning electron microscope (SEM, ZEISS Crossbeam 540). Roughness parameters of the surfaces were calculated based on the analysis of the AFM maps obtained by an Explorer microscope (Veeco Instruments). Electrochemical measurements were carried out, in simulated seawater electrolyte (3.5 wt.% NaCl solution) at room temperature, using a BioLogicSP-300. A standard three-electrode cell composed by a saturated

Ag/AgCl electrode as the reference electrode, a platinum wire as the counter electrode, and the prepared aluminium sample as the working electrode (exposed area = 1cm²), was

utilized as the working cell. After reaching the OCP, The potentiodynamic polarization curves were collected with a scanning rate of 0.2 mV/s.

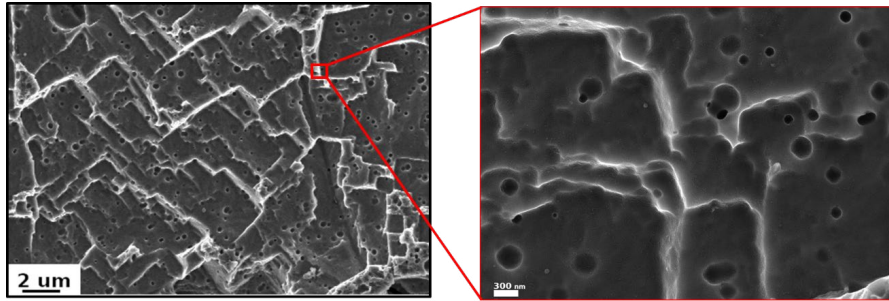


Fig.1 - Surface morphologies in original magnification of 20 kX and 200 kX

Fig.1 shows the surface scanning electron microscope (SEM) images of the treated sample surface. A high magnification of the surface morphology is also reported (x200,000).

The process of fabrication of the superhydrophobic surface comprises chemical etching and silane modification. In the experiment, the aluminium sample with static contact angle of about 70° is first etched in acid to obtain a hierarchical textured structure. Fish-like micro-scales with size of around 3 μm are formed. On these micro-protrusions, a regular nanometric pit population was also formed. These pits had the dimensions in the range of 80-150 nm. This bimodal structure considerably increased the effective

surface area and the roughness surface profile. This morphology is a consequence of the grain orientation and secondary phase's distribution. In fact, the aluminium alloy 6082 is characterized by Fe-Mn inclusions with micrometric dimensions randomly distributed on the whole surface. Moreover, numerous dislocations and defects are presents in the aluminium alloy matrix. These defects were more sensitive to the etching than other locations of the metal substrate [12]. At varying etching time, all the samples showed similar microstructure. In this context, a deep analysis of the nanostructure of these samples is mandatory to highlight the effect of the etching time.

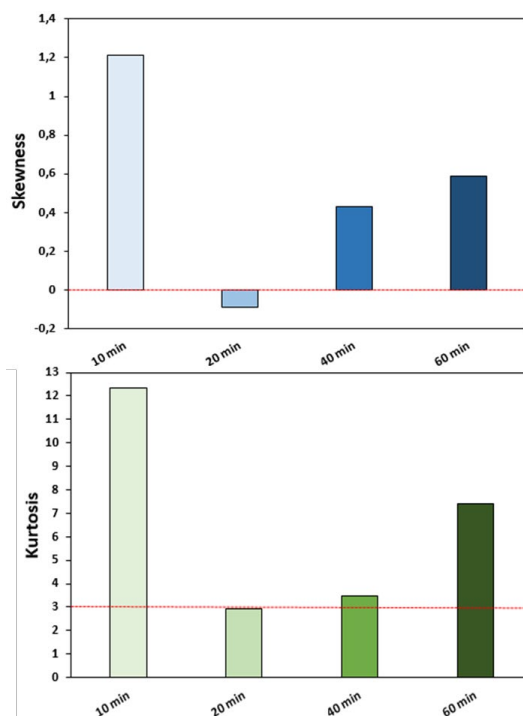


Fig.2 - Roughness parameters of etched samples

In order to better analyse the coatings' surface morphology, AFM scanning was performed on all samples and the surface roughness parameters were calculated based on the AFM mapping results and presented in Fig.2.

Two important parameters, Skewness and Kurtosis, were selected to evaluate the effect of the etching time on the surface morphologies. The skewness parameter, S_{sk} , is related to the degree of the symmetry of the variation in a profile about its mean line. $S_{sk} = 0$ if the distribution is symmetrical (equal repartition between peaks as valleys). $S_{sk} < 0$ indicates that the height distribution is skewed above the mean plane and it is related to a profile with deep valleys in smooth plateau such as porous structure. Conversely, a positive skewness parameter, height distribution skewed above the flatter average, is related to a profile characterized mainly with peaks and asperities. Finally, kurtosis, S_{ku} , measures the probability density sharpness of the roughness profile and its value is related to the degree of peakedness of a surface height distribution.

A S_{ku} value less than 3 indicates that the surface has relatively few peaks and low valleys, whereas a kurtosis value more than 3 indicates few valleys and many high peaks. When the kurtosis parameter is equal to 3, this indicates that the heights are characterized by a normal distribution (sharp and indented portions co-exist). In fact, the histograms of S_{sk} and S_{ku} against the etching time evidenced a dependence between these parameters. Indeed, the samples etched for 20 and 40 minutes are characterized by the closest to zero Skewness values indicating a quite symmetric distribution to zero. In addition, the peakedness of these samples (strongly dependent on the etching time) is near to 3, indicated a normal distribution of sharp and indented portions. In order to study the effect of the achieved morphologies on the wetting behaviour of the aluminium alloy samples, the water contact angles and the water sliding angles were measured.

Fig.3 shows the influence of changing the etching time on both water contact and sliding angles. It is clear that superhydrophobicity was initially enhanced by increasing the etching time, afterwards reduced after an etching time of one hour. In fact, the highest WCA (180°) and the lowest

WSA angles (0°) were obtained for the surfaces etched at 20 min and 40 min. The WCA rises by about 12.5%, from 160° to around 180° , and the WSA decreases from 30° to around 0° degrees when the etching time increases from 10 min to 20 min and 40 min. While all the aluminium specimens are superhydrophobic with a WCA higher than 150° , the difference in the wetting behaviour at increasing etching time is related to the diverse interactions of the silanized surface roughness with water (Cassie-Baxter or Wenzel state). In the Cassie-Baxter, the air-layer is able to significantly reduce the contact between the liquid and the surface, and thus the water droplet easily rolls off as on the case of the sample 20 min and 40 min samples. However, in the Wenzel state, the liquid droplet penetrates the surface grooves resulting in high adhesion and thus high sliding angle ($WSA > 90^\circ$). Consequently, the portion of air trapped in the solid/water interface is the key factor that controls the WCA and WSA and thus the anti-wetting surface type.

Our results point out that a transition between Wenzel and Cassie-Baxter states can be made by changing the etching time. The 10 min and 60 min samples are in a transitional state between Wenzel and Cassie-Baxter since the sliding angles are quite elevated (30° and 22° respectively) indicating that the air layer is not continuous (air is only partially entrapped into the surface valleys). However, the 20 min and the 40 min sample are Cassie-Baxter surfaces as indirectly identifiable by the low WSA ($0 \leq SA \leq 10^\circ$) which is probably due to the regular and homogeneous roughness that enhance the formation of a continuous air film following the Cassie-Baxter state (Fig.2). This result is consistent with the literature. In fact, Li et al. [13] demonstrated that the achievement of a high WCA and a low WSA on a solid surface requires a dual scale structure with a thin solid fraction. When the etching duration increases to one hour, the ordered nanostructure is destroyed that may negatively affect the air layer. Indeed, the air fraction trapped on the solid surface of the 60 min sample surface is probably lower than the 20 and 40 min samples resulting in lower WCA and higher WSA (Fig.3). Thus, at 60 min, the Cassie-Baxter state can break down and the inverse transition from Cassie-Baxter to Wenzel can occur.

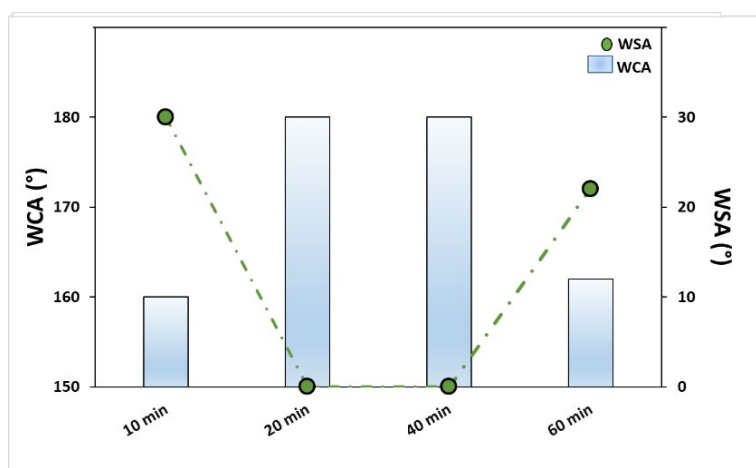


Fig.3 - Water contact angle (WCA) and water sliding angle (WSA) evolution with the etching time

Superhydrophobic surfaces with different water repellency behaviour were successfully elaborated. This reduction in the wettability of these surfaces may deeply affect their corrosion resistance. Thus, the corrosion resistance of the elaborated samples was investigated.

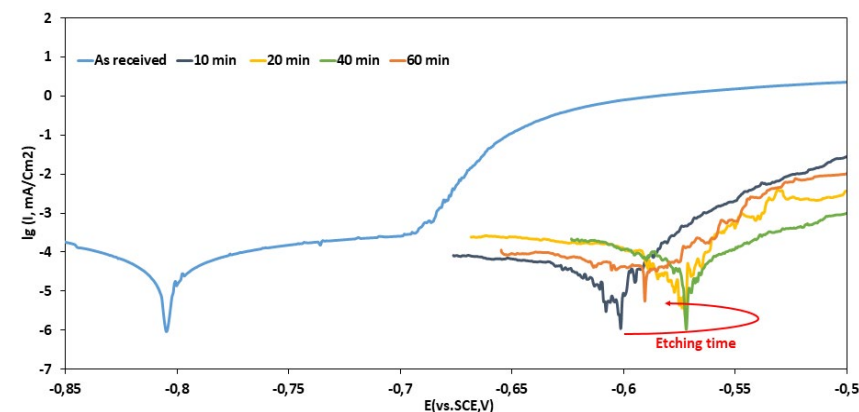


Fig.4 - Polarization curves of as received aluminium alloy and the superhydrophobic surfaces in seawater at room temperature

The electrochemical polarization test is a useful tool for assessing the corrosion behaviour of a solid surface. In a typical polarization curve, a high corrosion potential (E_{corr}) and a low corrosion current density (I_{corr}) corresponds to a good corrosion resistance.

The potentiodynamic polarization curves recorded for the as received aluminium alloy and superhydrophobic aluminium surfaces, having different WCA and WSA, in seawater (3.5 wt% NaCl solution) are presented in Fig.4. The corrosion potential (E_{corr}) and the corrosion current density

(I_{corr}) were calculated using the Tafel method.

As shown in Fig.4, the corrosion potential of the as-received sample is -805 mV vs. SCE. Following the surface modification, the corrosion potential E_{corr} shifted toward positive direction. In fact, E_{corr} positively increases from -805 mV to -601 mV for 10 min sample, to around -570 mV for both 20 min and 40 min samples and then decreases again to reach -589 mV for the 60 min sample. However, the surface treatment of the aluminium surface does not show significant modification of the corrosion current

density. These results are consistent with the wettability states. Indeed, the best corrosion results were obtained with the superhydrophobic surfaces following the Cassie-Baxter state (20 min and 40 min samples), thus, the superhydrophobic interface that reduces the interaction between the solution and the aluminium alloy surface enhances the

corrosion resistance of the samples. The trapped air on the hierarchical micro/nanostructures of the superhydrophobic aluminium surfaces acts as an "air cushion" inhibiting the penetration of corrosive ions (Cl^-) and leading to an improved corrosion protection [14].

CONCLUSIONS

Superhydrophobic surfaces were fabricated on aluminium alloy 6082 by coupling the modification of surface roughness, got by chemical etching, and the decrease of surface energy obtained by silane coating. The wettability state of these superhydrophobic surfaces varies with the etching time. In fact, the Cassie-Baxter state ($\text{WCA} \approx 180^\circ$ and $\text{WSA} \approx 0^\circ$) was achieved by a chemical etching for 20 and 40 minutes. On the other hand, a Wenzel state was obtained for the lowest and the highest etching times (10 min and 60 min). Thus, the wetting transitions from Wenzel to Cassie-Baxter can be managed by modifying the etching time. The wetting state alteration is based on the distribution of the roughness peaks and valleys. In addition, the as-modified aluminium surfaces revealed a good corrosion resistance behaviour in seawater compared with the as received one and the best results were obtained on the Cassie-Baxter surfaces. Thus, a normal distribution of peaks and valleys, especially in the nanostructure, is the key factor for obtaining the Cassie-Baxter state and thus for improving the wetting and the corrosion behaviour of the aluminium alloy.

REFERENCES

- [1] L. Zhai, M.C. Berg, F.Ç. Cebeci, Y. Kim, J.M. Milwid, M.F. Rubner, R.E. Cohen, Patterned superhydrophobic surfaces: Toward a synthetic mimic of the namib desert beetle, *Nano Lett.* 6 (2006) 1213–1217. doi:10.1021/nl060644q.
- [2] A. Khaskhoussi, L. Calabrese, E. Proverbio, Superhydrophobic Self-Assembled Silane Monolayers on Hierarchical 6082 Aluminum Alloy for Anti-Corrosion Applications, *Appl. Sci.* (2020) 1–14. doi:10.3390/app10082656.
- [3] G. Barati Darband, M. Aliofkhaezai, S. Khorsand, S. Sokhanvar, A. Kaboli, Science and Engineering of Superhydrophobic Surfaces: Review of Corrosion Resistance, Chemical and Mechanical Stability, *Arab. J. Chem.* (2018). doi:10.1016/j.arabjc.2018.01.013.
- [4] A. Khaskhoussi, L. Calabrese, E. Proverbio, An Easy Approach for Obtaining Superhydrophobic Surfaces and their Applications, *Key Eng. Mater.* 813 (2019) 37–42. doi:10.4028/www.scientific.net/KEM.813.37.
- [5] X. Gong, S. He, Highly Durable Superhydrophobic Polydimethylsiloxane/Silica Nanocomposite Surfaces with Good Self-Cleaning Ability, *ACS Omega*. 5 (2020) 4100–4108. doi:10.1021/acsomega.9b03775.
- [6] B. Majhy, R. Iqbal, A.K. Sen, Facile fabrication and mechanistic understanding of a transparent reversible superhydrophobic – superhydrophilic surface, *Sci. Rep.* 8 (2018) 1–11. doi:10.1038/s41598-018-37016-5.
- [7] L.A. Girifalco, R.J. Good, A theory for the estimation of surface and interfacial energies. I. Derivation and application to interfacial tension, *J. Phys. Chem.* 61 (1957) 904–909. doi:10.1021/j150553a013.
- [8] J. Jeevahan, M. Chandrasekaran, G. Britto Joseph, R.B. Durairaj, G. Mageshwaran, Superhydrophobic surfaces: a review on fundamentals, applications, and challenges, *J. Coatings Technol. Res.* 15 (2018) 231–250. doi:10.1007/s11998-017-0011-x.
- [9] U. Cengiz, C. Elif Cansoy, Applicability of Cassie–Baxter equation for superhydrophobic fluoropolymer–silica composite films, *Appl. Surf. Sci.* 335 (2015) 99–106. doi:10.1016/j.apsusc.2015.02.033.
- [10] G. Wang, S. Liu, S. Wei, Y. Liu, J. Lian, Q. Jiang, Robust superhydrophobic surface on Al substrate with durability, corrosion resistance and ice-phobicity, *Sci. Rep.* 6 (2016). doi:10.1038/srep20933.
- [11] A. Hooda, M.S. Goyat, J.K. Pandey, A. Kumar, R. Gupta, A review on fundamentals, constraints and fabrication techniques of superhydrophobic coatings, *Prog. Org. Coatings*. 142 (2020) 105557. doi:10.1016/j.porgcoat.2020.105557.
- [12] L. Calabrese, P. Bruzzaniti, E. Proverbio, Pitting corrosion of aluminum alloys in anhydrous ethanol, *Mater. Corros.* 69 (2018) 1815–1826. doi:10.1002/maco.201810125.
- [13] W. Li, A. Amirfazli, Microtextured superhydrophobic surfaces: A thermodynamic analysis, *Adv. Colloid Interface Sci.* 132 (2007) 51–68. doi:10.1016/j.cis.2007.01.001.
- [14] C. Liu, F. Su, J. Liang, Facile fabrication of a robust and corrosion resistant superhydrophobic aluminum alloy surface by a novel method, *RSC Adv.* 4 (2014) 55556–55564. doi:10.1039/c4ra09390a.